Egyptian Journal of Chemistry

http://ejchem.journals.ekb.eg/

Pristine and Nickel Doped Bismuth Vanadate Nanopowder For p-Nitrophenol Degradation under UV Light Irradiation

N. Karthi[1]; K. A. Ramesh kumar [2]; P. Maadeswaranc[3]

[1]*Research Scholar, Department of Energy Studies, Periyar university, Salem – 636 011, Tamilnadu, India.*

[2]*Associate Professor & Head, Department of Energy Studies, Periyar university, Salem – 636 011, Tamilnadu, India.*

[3]*Assistant Professor, Department of Energy Studies, Periyar university, Salem – 636 011, Tamilnadu, India.*

Abstract

The current work outlines the breakdown of p-($C_6H_5NO_3$) utilizing pure and various concentrations of $BiVO_4$/Ni hybrid material prepared by the precipitation method. The composition and surface structure investigations were studied using several techniques such as XRD, and SEM coupled to EDAX spectroscopy. The hybrid material presented absorption edge of 2.5 to 2.87 eV was calculated through the computation of the KM function employed to diffuse reflectance spectrophotometry data. Ultraviolet–Visible spectral analysis was carried out to screen the breakdown of p-($C_6H_5NO_3$) and the development of secondary products. The application of pure and $BiVO_4$/Ni-based photo catalyzer reduce the amount of carbon after the breakdown of p-($C_6H_5NO_3$). Depends upon the outcomes acquired in the studies, pure and Ni doped Bismuth vanadate (3%, 5% and 7%) has end up being an optimistic material appropriate to eliminate contrary chemicals in water treatment plants.

Keywords: $BiVO_4$; Nickel doped $BiVO_4$; p-Nitropheonol; Photo-degradation.

1. Introduction

Nanotechnology provides various chances to inhibit, to decrease and to sense the habitat pollutions. It has been accounted extensively that the present ecological issues could be determined or incredibly decreased by the use of nano-catalysts, bio-active nanoparticles, nano-structured catalytic membranes, submicronic NPs, nano-powder, bio-nano-composites, nano-tubes, magnetic NPs, magnetic nano-composites, grains, chips etc [1-5]. Semiconductor NPs have gained significant consideration owing to their distinctive characteristics and their probable applications in different sectors of science. In recent years, researchers have focused mainly for the evolution of effective strategies to synthesize NPs based on metals with chosen surface structure and dimensions. Green synthesis of NPs includes the major use of safer (non-toxic) chemicals, renewable materials and environment friendly solvents which is a major issue that should be taken into consideration. In this regard, the bismuth vanadate has gained more focus due to their magnificent physical and chemical characteristics like ferro-elasticity and photo-chromism [6]. During the modern years, bismuth vanadate being a visible-light determined photo-catalyst has been analyzed widely for the cleavage of H_2O molecules, the conversion of CO_2 into C_2H_5OH in H_2O by reduction and the removal of natural contaminants such as methyl orange, rhodamine and phenol under visible light irradiation. Mingming Yao *et al* [2013] reported the synthesis of monoclinic scheelite mesoporous $BiVO_4$ by an impregnated template method [7]. Bismuth nitrate pentahydrate &

*Corresponding author e-mail: karameshkumar77@gmail.com
Receive Date: 28 May 2021, Revise Date: 10 August 2021, Accept Date: 11 October 2021
DOI: 10.21608/EJCHEM.2021.77859.3812

ammonia meta vanadate were respectively used as Bi and V predecessor, and mesostructured silicon dioxide aero-gel was utilized as a rigid template. Meysam Tayebi *et al* [2018] narrate Molybdenum (Mo)/Mono-clinic $BiVO_4$ catalysts were assembled through simple dip-coating method [8]. Vandana Yadav *et al* [2019] narrate photodegradation of Nitrophenol with boron doped titanium dioxide exhibited maximum degradation efficiency (88%) as compared to pristine titanium dioxide (78%) [9]. In this present work, Ni doped $BiVO_4$ (Ni at. 3, 5 and 7%) nanoparticles were examined and morphological and optical properties of doped systems and the samples synthesized were characterized using several characterizations such as X-ray Diffractive spectroscopy, Scanning Electron Microscopy-Energy Dispersive X-ray Analysis, Fourier Transform-Infra-Red Spectroscopy and Ultraviolet-Differential Reflectance Spectroscopy and the results are deliberated on the light to practice these nanoparticles for photo-degradation of p-Nitrophenol.

2. Experimental details

2.1. Materials and methods

The following materials were employed: $(Bi(NO_3)_3.5H_2O$ – Bismuth Nitrate pentahydrate (Sigma Aldrich 98%), Ammonium Meta vanadate {(NH_4VO_3) HIMEDIA 98 - 102%}, Nickel-nitrate ($NiNO_2$), PVP (HIMEDIA), NaOH pellets and de-ionised water. In the present work, the synthesis of Nickel doped $BiVO_4$ NPs were prepared by precipitation method [9]. The analytical grade (AR) ammonium meta vanadate, bismuth nitrate and nickel nitrate were used as starting materials. In the standard process of synthesis which was shown in fig 1, the stoichiometric amount of 1.40376 g NH_4VO_3 and the 2.91042 g of $Bi(NO_3)_3.5H_2O$ were dissolved in 20 ml of de-ionised water together with stirring. By addition of concentrated hydrochloric acid (HCl) to the aqueous solution, the pH was balanced approximately to 9.0. The prepared solutions were combined together quickly to generate a homogenous mixture. To the above mixture, 0.15 g of PVP was added drop wise over 20 min at room temperature. Then, a required quantity of sodium hydroxide was mixed to the above precursor solution with constant stirring at 60^{o}C for about 24 h. Then, the reactants were added in the order given in fig.1 and stirring continues for about some time till the colour of the solution changed to yellow. Then, the obtained yellow color precipitate was collected and washed with acetone, ethanol, methanol and 20 ml of de-ionized water. As well the precipitated compound was dried for about 4 hours at the temperature of 60°C and it is grinded moderately. In the end, muffle furnace was used to heat the above products with 5^{o}C/min heating rate under the air atmosphere at 450^{o}C for about 2 h and cooled to room temperature. By using the same procedure and distinct doping source materials, the synthesis of Ni doped $BiVO_4$ with different dopant concentrations (3, 5 and 7%) were carried out. Besides, the prepared samples were subjected to characterization through several methods like XRD, Scanning Electron Microscopy-EDAX, FTIR, and Ultraviolet-Differential Reflectance Spectroscopy.

2.2. Photodegradation of p-Nitrophenol

A stock solution was prepared by dissolving p-Nitrophenol in distilled water along with synthesized photo-catalyst which is then exposed to UV–Vis light and monitored under UV–Vis spectrophotometer [10]. A 50 mL of 10 ppm concentrated p-Nitrophenol solution was added to 40 mgs of photo-catalyst and then the prepared solution was kept in dark for about 15 minutes and then exposed to ultraviolet-visible lamp for dye degradation [11]. To eliminate the photo-catalyst particles, the sample was taken at a particular time interval and immediately centrifuged for 10 minutes. Finally, the sample absorbance was evaluated under ultraviolet spectrophotometer. The photocatalytic degradation efficiency [12] was calculated using below equation,

$$[(C_0\text{-}C)/C_0] \times 100 = [(A_0 – A/A_0)] \times 100 \quad (1)$$

From the equation, C_0 represented the initial dye concentration, while C denoted the dye concentration on each interval in terms of time. Meanwhile, A_0 stood for the initial absorbance and A referred to the absorbance.

Fig.1. Synthesis of Ni doped $BiVO_4$ (3, 5 and 7 %) Nanoparticles

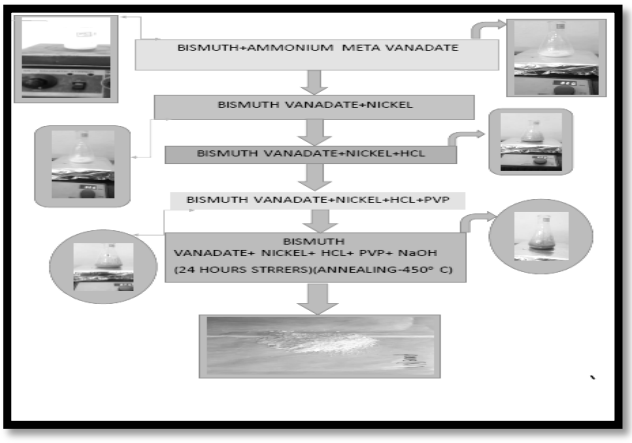

3. Results and Discussion

3.1. X-Ray Diffraction - Structural analysis

The formation of well orthorhombic structures at both the durations of precipitation treatment was observed in XRD spectra of the synthesized pure $BiVO_4$ and Nickel doped Bismuth vanadate (3, 5 & 7 %) nanoparticles in fig. 2. The graphs obtained were in correlation with JCPDS card No. 12-0293 as shown in Fig.2, which corresponded to space group of orthorhombic bismuth vanadates with a= 5.326, b= 5.056 and c= 12.00[13]. Although, notable differences were observed upon Ni doping. An occurrence of interstitial doping of Ni on $BiVO_4$ was evident from XRD spectra, which displayed additional Ni peaks, along with characteristic orthorhombic peaks of $BiVO_4$. Four distinct diffraction peaks were located and they were matched well with the (112), (113), and (024) planes without any impurity phase, demonstrating the high purity of the samples.

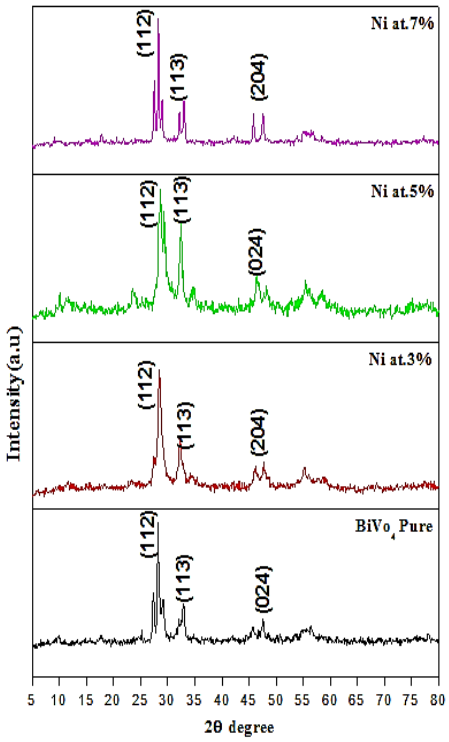

Fig.2. XRD of synthesized Pure Bismuth vanadate and Nickel doped Bismuth vanadate (3, 5 and 7 %) NPs

3.2. SEM analysis

Surface morphology of pure $BiVO_4$ and Nickel-doped $BiVO_4$ (3, 5 and 7 %) nanoparticles [14] were shown in Fig.3. In order to remove the impurities, the synthesized NPs were subjected to annelation as they were distributed uniformly with small sized grains resembled the nano dots. This might be due to the formation of cluster particles. The fusion of cluster was observed at some region. The SEM image had been recorded at 10µm resolution. As the doping level was increased, the bigger ionic radii of Ni ions distorted the crystal structures due to mismatching of ionic radii which increased the grains/particles growth activity of $BiVO_4$ and formation of bigger particles.

Table 1 Structural parameters of pure and various concentration of Ni doped $BiVO_4$ samples at 450°C for 2 hours

$BiVO_4$ (where x=0, 3, 5, and 7%)	2θ (degree)	hkl	d-spacing (nm)	FWHM (degree)	Grain size (D) nm	Dislocation density (10^{14} lines/m^2)	Micro-strain (ε) $10^4 lin^{-2}m^{-4}$
	28.2065	112	3.16124	0.33630	24.3683	0.001684	0.176737
00	32.8787	113	2.72191	0.49750	15.0648	0.003604	0.170670
	45.6782	204	1.98457	0.51020	11.9354	0.003500	0.178952
	28.4939	112	3.13001	0.80150	10.2311	0.009553	0.145005
03	33.0000	113	2.71218	0.50900	07.9357	0.003770	0.170107
	46.2000	204	1.96336	1.00000	05.6385	0.013395	0.159175
	28.8979	112	3.08716	1.72080	04.7696	0.043956	0.083537
05	32.3975	113	2.76123	1.07500	12.5348	0.016870	0.135511
	46.5541	204	1.94925	1.04170	07.9118	0.014497	0.157831
	28.2808	112	3.15311	0.28970	28.2927	0.001249	0.100029
07	33.0005	113	2.71214	0.33870	17.0413	0.001670	0.180142
	45.7987	204	1.97963	0.82370	10.8772	0.001179	0.187856

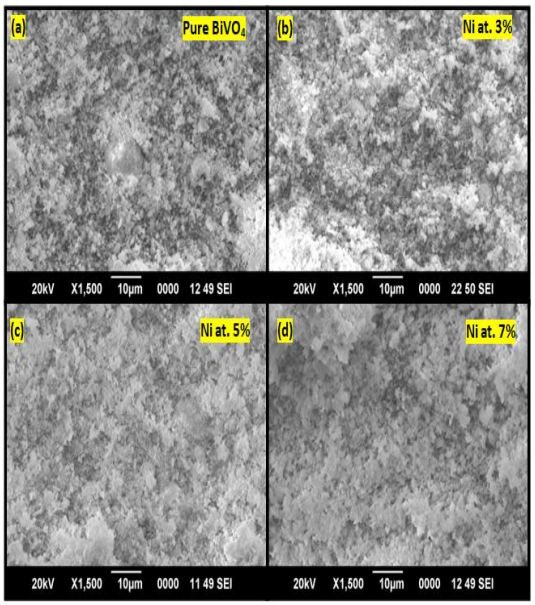

Fig 3. SEM images of synthesized (a) pure $BiVO_4$, (b) 3% Ni doped $BiVO_4$, (c) 5% Ni doped $BiVO_4$ and (d) 7% Ni doped $BiVO_4$ NPs

3.3. EDAX analysis

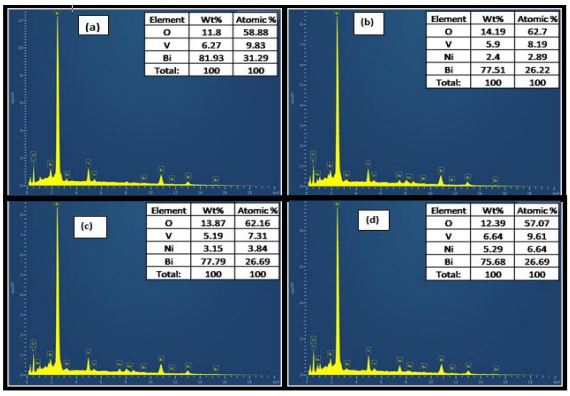

Fig 4. EDAX spectra of synthesized (a) pure $BiVO_4$ (b) 3% Ni doped $BiVO_4$, (c) 5% Ni doped $BiVO_4$ (d) 7% Ni doped $BiVO_4$ nanoparticles.

Compositional characterization [15] of Ni-doped $BiVO_4$ NPs was studied using Energy-Dispersive X-ray analysis. The atomic percentage of doped materials is 2.89, 3.84 and 6.64. Besides the adaptive values of dopant concentrations, their homogeneous distribution in the $BiVO_4$ substance was also deliberated. Figure 4 indicated the composition of the synthesized NPs evaluated by Energy-Dispersive X-ray analysis.

3.4. UV-Vis Diffuse Reflectance Spectral and Band-gap Analysis

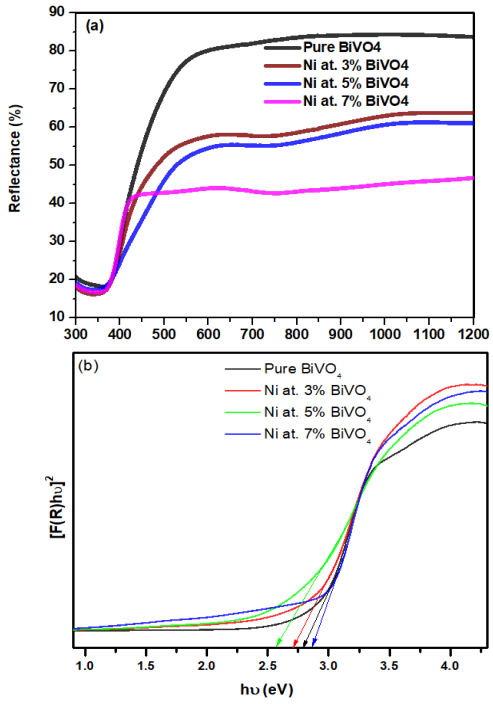

Fig. 5 (a) Diffuse reflection spectra, (b) Optical Band-gap plots of $BiVO_4$ and various concentration of Ni doped $BiVO_4$ NPs

Fig.5 (a) shows the diffuse reflectance spectra of pure and Ni-doped samples measured in the wavelength range of 400-500 nm with UV–Visible spectro-photometer. The distinguished peak in the reflectance spectra was reduced below 400 nm, which was due to with band-to-band absorption of pure and Nickel doped bismuth vanadate. Additionally, there was a broad decrease in wavelength near 500 nm was also detected for the pure and Nickel doped bismuth vanadate, which was ascribed owing to the intrinsic defect absorption. The direct band-gap of pure and Ni doped substance was deliberated using Kubelka-Munk function [16] mentioned as follows:

$$\alpha = (1-R)^2/2R \qquad (2)$$

Where, α is the absorption coefficient & R is the reflectance. The absorption band gap energy can be inspected by the equation mentioned below.

$$(\alpha h\nu)^n = B\,(h\nu - Eg) \qquad (3)$$

Where, $h\nu$ - the photon energy, α - the absorption coefficient, B - a constant to the content and the value of n relies upon the nature of transition. The bandgap values of pure and Ni samples were found to be 2.8, 2.72, 2.57, and 2.87 eV and it was shown in Fig.5 (b). While increasing the concentration, the band-gap increase from 2.5 to 2.87 eV. The energy of band gap also changed, which is due to variations in the grain size of $BiVO_4$.

3.5. *Photodegradation of p-Nitrophenol Using Pure and 3% , 5% and 7% of Ni doped $BiVO_4$*

As shown in Fig.6, under UV light, p-Nitro-phenol solution was irradiated in the presence of pure and Ni-doped $BiVO_4$ (3%,5% and 7%) nanoparticles, a decrease in the concentration of p-($C_6H_5NO_3$) was noticed during the 75 minutes and then remained constant. The decrease in the concentration of p-($C_6H_5NO_3$) at initial stage was owing to adsorption on Ni-doped $BiVO_4$ nanoparticles. Further, in the presence of pure and Ni-doped $BiVO_4$ nanoparticles under UV irradiation had led to increase in p-Nitrophenol of about 61-81%. The effect of pH on photocatalytic breakdown was studied initially for the pH of 5, 7, 9, and 11 under the certain conditions such as 40 ppm of p-Nitrophenol, catalyst loading = 10 ppm. Commonly, the photo-degradation mechanism comprised of the excitation by H^+ with energy equal to or more than the band-gap of NPs monitored by charge separation and migration caused in the surface reactions of oxidation and reduction. Below Ultra Violet radiation, excitation of a H+ of energy larger than or equal to a band-gap of Ni –

doped $BiVO_4$, (e−) would move from the valence band to conduction band, important to the development of the same number of h^+ in the valence band.

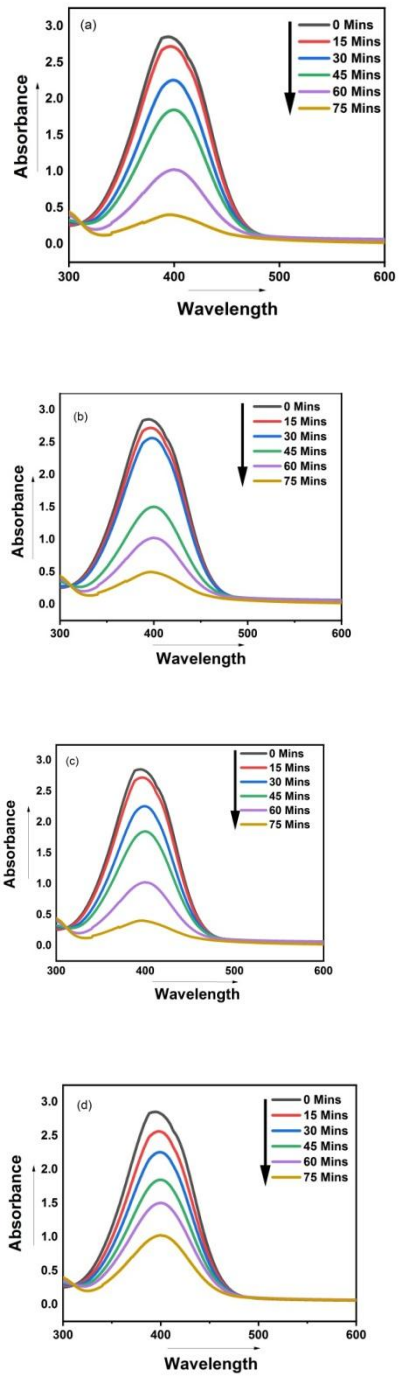

Fig.6. Photodegradation of p-Nitropheonol using (a) Pure $BiVO_4$ and (b) 3% Ni doped $BiVO_4$ (c) 5% Ni doped $BiVO_4$ and (d) 7 % Ni doped $BiVO_4$

$$\text{Ni} - \text{doped BiVO}_4 + h\nu \longrightarrow h^+_{(VB)} + e^-_{(CB)} \quad (4)$$

When adsorbed H_2O or hydroxide anion reacted with h^+ (VB), hydroxyl radicals were formed.

$$h^+ + H_2O \longrightarrow {}^{\cdot}OH + H^+ \quad (5)$$

$$H^+ + OH^- \longrightarrow {}^{\cdot}OH \quad (6)$$

Super-oxide anion radicals were generated when the e^- in conduction band reacted with free radical of oxygen molecule.

$$e^- + {}^{\cdot}O_2 \longrightarrow O_2 \quad (7)$$

From the above equation, it is confirmed that the reactive radicals like hydroxide and oxygen played a significant part in the photo-degradation of p-Nitrophenol [17].Fig.7 shows the mechanism p-Nitrophenol degradation.

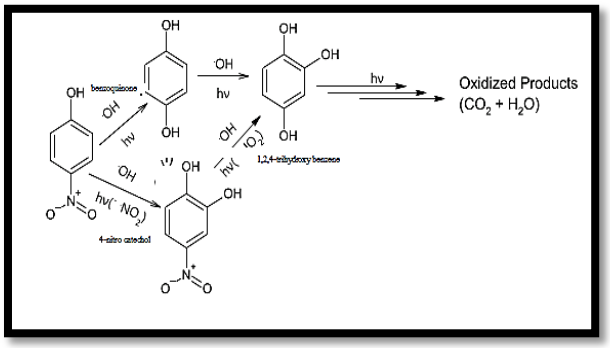

Fig. 7. Mechanism of p-Nitropheonol degradation

The photodegradation efficiency of nanomaterials was calculated by the following formula

$$D\ (\%) = (A_0 - A_t) / (A_0)\ x\ 100 \quad (8)$$

Where,
D - The degradation efficiency (in %).
A_0 - is the UV absorption of dye with sun light irradiation time (0 min) and
A_t - is the UV absorption of dye after UV-light irradiation (t-min).
The Photo degradation efficiency of pure and Ni doped $BiVO_4$ (3, 5 and 7%) nanoparticles were found to be 61%, 74%, 79% and 81%.

3.6. Stability and Reusability of Photocatalyst

The reusability of the $BiVO_4$ and Ni-doped $BiVO_4$(3, 5 and 7%) photocatalysts were investigated by repeating p-NP degradation experiments five times. The results indicate prepared catalysts are stable and reusable. Also, it indicates that the photocatalytic efficiency of Bismuth vanadate and Nickel doped Bismuth vanadate (3, 5 and 7%) nanoparticles were

decreased slowly and then stable. There is slight change in the degradation efficiency of $BiVO_4$ and Ni-doped $BiVO_4$ (3, 5 and 7%) after second run. Thus, suggests that $BiVO_4$ and Ni-doped $BiVO_4$ (3, 5 and 7%) photocatalysts have excellent stability and reliability for photodegradation of pollutants.

Table 2
Comparison between the synthesized photocatalysts with the various literatures for p-nitrophenol degradation

Photocatalyst	Light Source	Time in Mins	Efficiency	Ref
Pure $BiVO_4$	UV	75	61%,	This Work
3% Ni/$BiVO_4$	UV-	75	74%,	This Work
5% Ni/$BiVO_4$	UV	75	79%	This Work
7% Ni/$BiVO_4$	UV	75	81%.	This Work
Cu/$BiVO_4$	white LED	60	35%	[19]
Ag_3PO_4	Visible	45	51.2%	[20]
Cu_2O/TiO_2	UV	180	39.5%	[21]
TiO_2	UV	120	40%	[22]
ZnO	UV	150	80%	[23]
Fe_2O_3/FeS	UV	150	98%	[24]
Ag/AgBr	Visible	180	96%	[25]

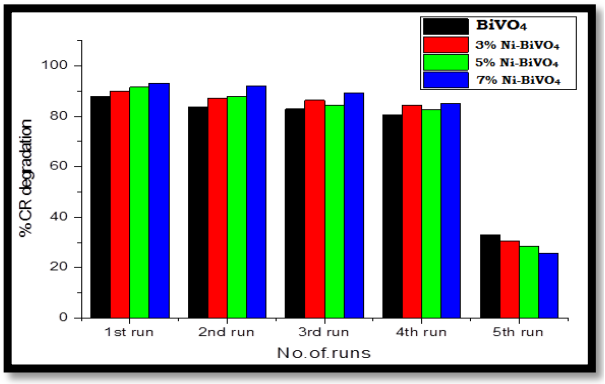

Figure 8 Effect of reusability: [p-NP] = 1 x 10^{-4} M, catalyst loaded 0.10 g/50mL, pH-9, irradiation time-75 min

3.7. Comparison of Synthesized Photocatalyst

By associating the outcomes of our current work and other investigations report, one can realize that the pure $BiVO_4$ and Ni doped $BiVO_4$ photocatalysts showed enhanced photocatalytic enactment for the degradation of p-Nitrophenol below UV- light irradiation. Table 2 shows comparison between the synthesized pure $BiVO_4$, various concentrations of Ni doped $BiVO_4$ photocatalyst and the various literatures reported for photo-degradation of nitrophenol. Furthermore, several of these investigation reports used Ultraviolet or visible-light as the light-source. It can be seen that photo-catalyst of pure $BiVO_4$ and Ni doped $BiVO_4$ shows the best p-Nitrophenol degradation activity

4. Conclusion

This investigation described the growth of a new hybrid and Ni doped $BiVO_4$ (Ni at. 3, 5 and 7%) nanoparticles and their effective preparation and characterization. XRD pattern revealed the orthorhombic structure and the average crystallite size was 10-24 nm for pure and Ni doped $BiVO_4$ (Ni at. 3, 5 and 7%). SEM clarifications exposed the morphology of the synthesized undoped $BiVO_4$ and Ni-$BiVO_4$ NPs which were detected to be Nano clusters. EDS examination endorsed the pureness of synthesized undoped $BiVO_4$ and Ni doped $BiVO_4$ NPs. While increasing concentration of Ni into $BiVO_4$ system, the bandgap increased from 2.5 to 2.87 eV. The Photo degradation efficiency of pure and Ni doped $BiVO_4$ (3, 5 and 7%) nanoparticles were found to be 61%, 74%, 79% and 81%.

5. Conflicts of interest

There are no conflicts to declare.

6. Acknowledgments

Deep thanks to Dr. K. A. Rameshkumar, Associate Professor & Head, Department of Energy Studies, Periyar university and Dr. P. Maadeswaran, Assistant Professor, Department of Energy Studies, Periyar university for their valuable guidance and support.

7. References

[1] Guerra F.D., Attia M.F., Whitehead D.C. and Alexis F., Nanotechnology for Environmental Remediation. *Materials and Applications. Molecules*, **23**(7), 1760(2018).
[2] Nusrat Shaheen., Muhammad Asif Yousuf., Imran Shakir., Sonia Zulfiqar., Philips Olaleye Agboola., and Muhammad Farooq Warsi., *Physica B: Condensed Matter*, **580**, 411820(2020).
[3] Cotica L.F. *et al*. Fungal Nanobionics: Principles and Applications; *Nanobiocomposites: Synthesis and Environmental Applications*, Springer, Singapore, p. 1-19(2018).
[4] Abbad S., Guergouri K., Gazaout S., Djebabra S., Zertal A., Barille R. and Zaabat M., *Journal of Environmental Chemical Engineering*, **8**(3), 103718(2020).
[5] Sajjadi M., Nasrollahzadeh M. and Reza Tahsili M., *Separation and Purification Technology*, **227**, 115716(2019).

[6] Chaudhuri A., Mandal, Chi X., Yang M., Scott M.C., Motapothula M. *et al*. *Phys. Rev. B*, **97**, 195150(2018).
[7] Yao M., Liu M., Gan L., Zhao F., Fan X., Zhu D. *et al*. Monoclinic mesoporous $BiVO_4$: Synthesis and visible-light-driven photocatalytic property. *Colloids and Surfaces A: Physicochemical and Engineering Aspects*, **433**, 132-138(2013).
[8] Tayebi M., Tayyebi A. and Lee B. K., Photocharged molybdenum-doped $BiVO_4$ photoanodes for simultaneous enhancements in charge transport and surface passivation. *Solar Energy*, **191**, 427-434(2019).
[9] Karthi N., Rameshkumar K.A. and Maadeswaren P., *Journal of Ovonic Research*, **16**(1), 119–126(2019).
[10] Martimiano do Prado T., Lindo Silva F., Grosseli G., Sergio Fadini P., Fatibello-Filho O. and Cruz de Moraes F., Using $BiVO_4$/CuO-Based Photoelectrocatalyzer for 4-Nitrophenol Degradation. *Materials*, **13**, 1322(2020).
[11] Yang L., Chen C., Hu Y., Wei F., Cui J., Zhao Y., *et al*. *Journal of Colloid and Interface Science*, **562**, 21-28(2020).
[12] Ammar I., Gassoumi A., Akkari A., Delpech F., Ammar S., and Turki-Kamoun, N., *The European Physical Journal Plus*, **13**, 410(2019).
[13] Kong D., Qi J., Liu D. *et al*. Ni-Doped $BiVO_4$ with V4+ Species and Oxygen Vacancies for Efficient Photoelectrochemical Water Splitting. *Trans. Tianjin Univ.*, **25**, 340–347 (2019).
[14] Walid A., Soeparman S., Wahyudi S., and Sasongko M.N., The effect of nickel doped Bismuth Vanadium Oxide on microstructures and electric properties towards $BiVO_4$-NiO composite. *Materials Chemistry and Physics*, **265**, 124452(2021).
[15] Chhabilal Regmi., Dipesh Dhakal and Soo Wohn Lee, *Nanotechnology*, **29**, 064001(2018).
[16] Tangcharoen T., T-Thienprasert J. and Kongmark C., Effect of calcination temperature on structural and optical properties of MAl2O4 (M = Ni, Cu, Zn) aluminate spinel nanoparticles. *J Adv Ceram*, **8**, 352–366(2018).
[17] Graus J., Bueno-Alejo C.J. and Hueso J.L., In-Situ Deposition of Plasmonic Gold Nanotriangles and Nanoprisms onto Layered Hydroxides for Full-Range Photocatalytic Response towards the Selective Reduction of p-Nitrophenol. *Catalysts*, **8**, 354(2018).
[18] Guerra F.D., Attia M.F., Whitehead D.C. and Alexis F., Nanotechnology for Environmental Remediation. *Materials and Applications. Molecules*, **23**(7), 1760(2018).
[19] Martimiano do Prado T., Lindo Silva, F., Grosseli, G., Sergio Fadini P., Fatibello-Filho O., Cruz de Moraes F., Using BiVO4/CuO-Based Photoelectrocatalyzer for 4-Nitrophenol Degradation. *Materials*, **13**, 1322(2020).
[20] Yang Li., Xinyan Xiao., Zhihao Ye., Fabrication of BiVO4/RGO/Ag3PO4 ternary composite photocatalysts with enhanced photocatalytic performance. *Applied Surface Science*. **467,** 902(2019).
[21] Lixia Yang., Shenglian Luo., Yue Li., Yan Xiao., Qing Kang., and Qingyun Cai., High Efficient Photocatalytic Degradation of p-Nitrophenol on a Unique Cu2O/TiO2 p-n Heterojunction Network Catalyst. *Environmental Science & Technology* **44** (19), 7641(2010).
[22] Shun-xing Li., Feng-ying Zheng., Xian-li Liu., Feng Wu., Nan-sheng Deng., Jian-hong Yang., Photocatalytic degradation of p-nitrophenol on nanometer size titanium dioxide surface modified with 5-sulfosalicylic acid. *Chemosphere*. **61(4),** 589-594(2005),
[23] Sugiyama M., Salehi Z., Tokumura M., KawaseY., Photocatalytic degradation of p-nitrophenol by zinc oxide particles. *Water Sci Technol* **65**(10), 1882–1886(2012).
[24] Pouretedal HR., Tavakkoli M., (2013) Photodegradation of para-nitrophenol catalyzed by Fe2O3/FeS nanocomposite, *Desalination and Water Treatment*. **51(**24), 4744-4749(2012).
[25] Tingting Li., Shenglian Luo., Lixia Yang., Microwave-assisted solvothermal synthesis of flower-like Ag/AgBr/BiOBr microspheres and their high efficient photocatalytic degradation for p-nitrophenol. *Journal of Solid State Chemistry*, **206**, 308-316(2013).